

A Localized Tolerance in the Substrate Specificity of the Fluorinase Enzyme enables “Last-Step” ^{18}F Fluorination of a RGD Peptide under Ambient Aqueous Conditions**

Stephen Thompson, Qingzhi Zhang, Mayca Onega, Stephen McMahon, Ian Fleming, Sharon Ashworth, James H. Naismith, Jan Passchier, and David O'Hagan*

Abstract: A strategy for last-step ^{18}F fluorination of bioconjugated peptides is reported that exploits an “Achilles heel” in the substrate specificity of the fluorinase enzyme. An acetylene functionality at the C-2 position of the adenosine substrate projects from the active site into the solvent. The fluorinase catalyzes a transhalogenation of 5'-chlorodeoxy-2-ethynyladenosine (CIDEA) to 5'-fluorodeoxy-2-ethynyladenosine (FDEA). Extending a polyethylene glycol linker from the terminus of the acetylene allows the presentation of bioconjugation cargo to the enzyme for ^{18}F labelling. The method uses an aqueous solution (H_2^{18}O) of [^{18}F]fluoride generated by the cyclotron and has the capacity to isotopically label peptides of choice for positron emission tomography (PET).

The fluorinase enzyme, originally isolated from *Streptomyces cattleya*, catalyzes the reaction between S-adenosyl-L-methionine (AdoMet, **1**) and fluoride to form 5'-fluoro-5'-deoxyadenosine (FDA, **2**) and L-methionine (L-Met, **3**), as illustrated in Scheme 1 a.^[1] The enzyme has found application in positron emission tomography (PET) as a result of its ability to catalyze C– ^{18}F bond formation in the presence of [^{18}F]fluoride as the nucleophile.^[2] The enzymatic process has a technical advantage in the PET context because [^{18}F]fluoride is generated in the cyclotron as a dilute solution in [^{18}O]water, and the enzyme can use this form of aqueous fluoride directly. This feature obviates the usual requirement to secure dry [^{18}F]fluoride by ion-exchange chromatography

and as a Kryptofix 222 formulation.^[3] The enzymatic process therefore offers the possibility to directly radiolabel biomolecules in the aqueous phase.

A major constraint of fluorinase-based technology is that the enzyme has high substrate specificity. To date, ^{18}F -radiolabelled compounds using the fluorinase enzyme have been prepared from [^{18}F]FDA (**2**), the product of the native enzymatic reaction.^[4–6] However, there is some substrate tolerance for halide substituents. It has been shown that 5'-chloro-5'-deoxyadenosine (CIDA, **4**) is a better substrate than FDA (**2**) for the generation of AdoMet (Scheme 1 b).^[7] This is because chloride is a better leaving group than fluoride, but is a poor nucleophile in the forward reaction. Also in these reactions L-selenomethionine (L-SeMet) is a better substrate than L-Met (**3**), generating AdoSeMet (**5**) in place of AdoMet (**1**). More generally, the substrate specificity of the fluorinase enzyme is poor. All carbon skeletal modifications that have been explored so far lead to substantially slower kinetics, frustrating efficient biocatalysis. Herein we report a breakthrough in substrate specificity which exploits a structural modification to the substrate, incorporating an acetylene moiety at the C-2 position of the adenine ring. Close inspection of co-crystal structures of the fluorinase enzyme with FDA (**2**, Figure 1)^[8] indicated that the hydrogen atom at the C-2 position of adenine was positioned in the active site close to the enzyme surface and it was envisaged that a small linear functional group at the C-2 position should extend outwards into the solvent. It appeared most strategic to place an acetylene functionality at the C-2 position because of its linearity and low steric influence. Thus 5'-chloro-5'-deoxy-2-ethynyladenosine (CIDEA, **6**) became a candidate substrate for a transhalogenation reaction. The route developed for the synthesis of **6** is outlined in Scheme 2. Iodoadenosine **10**, prepared from guanosine **9**,^[9,10] was subject to Sonogashira cross-coupling with trimethylsilylacetylene to generate **11** and introduce the acetylene functionality. Trimethylsilyl-protected ethynyladenosine (**11**) was then converted into the required compound **6** in a one-pot procedure.^[11] A sample of 5'-fluorodeoxy-2-ethynyladenosine (FDEA, **8**), the anticipated product of enzymatic transhalogenation, was also prepared as a reference compound by protection of the 2',3'-diol of **11** as an acetonide, fluorination^[12] of the primary alcohol, and subsequent hydrolysis (Scheme 2).

FDEA (**8**) was also subjected to co-crystallization trials with the fluorinase enzyme and a single-crystal X-ray structure was solved to 2.4 Å by molecular replacement using the historical fluorinase refinement.^[8] The overlay of

[*] S. Thompson,^[†] Q. Zhang,^[†] S. McMahon, J. H. Naismith, D. O'Hagan
School of Chemistry
University of St Andrews
North Haugh, St Andrews, KY16 9ST (UK)
E-mail: do1@st-andrews.ac.uk

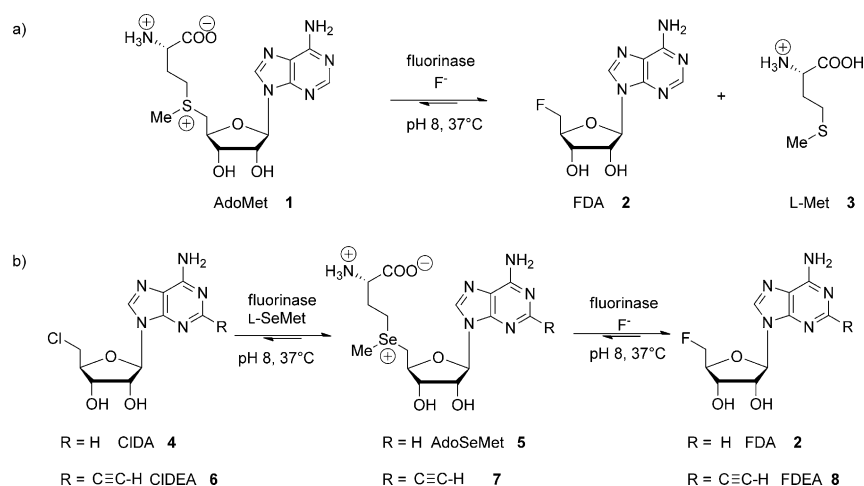
M. Onega, S. Ashworth, J. Passchier
Imanova, Burlington Danes Building
Imperial College London, Hammersmith Hospital
Du Cane Road, London, W12 0NN (UK)

I. Fleming
Aberdeen Biomedical Imaging Centre
School of Medicine and Dentistry, University of Aberdeen
Foresterhill, Aberdeen, AB25 2ZD (UK)

[†] These authors contributed equally to this work.

[**] We thank the ERC, EPSRC and the Scottish Imaging Network (SINAPSE) for grants, and the John and Kathleen Watson Scholarship (S.T.) for financial support.

Supporting information for this article is available on the WWW under <http://dx.doi.org/10.1002/ange.201403345>.



Scheme 1. Selected fluorinase-catalyzed reactions of AdoMet (**1**), CIDA (**4**), and CIDEA (**6**).

a) Transformation of **1** to FDA (**2**) and L-methionine (**3**). b) Transhalogenation of **4** (or **6**) and L-selenomethionine to **2** (or FDEA **8** from **6**), via intermediates **5** (or **7**).

see Figure S1b in the Supporting Information). This transhalogenation demonstrated that the enzyme does indeed have a specificity weakness at the C-2 position of adenine. With this result in mind, it became immediately attractive to explore extending a polyethylene glycol (PEG) chain from the terminus of the acetylene, as a tether onto which a cargo, such as a peptide, could be attached, as a potential strategy for radiolabelling the peptide cargo with fluorine-18. RGD peptides (RGD = arginylglycylaspartic acid) are validated ligands with high affinity for $\alpha_v\beta_3$ integrin epitopes on the surface of a variety of cancer cells.^[13] These peptides have been the focus of many labelling studies for PET in the development of tumor-imaging agents for the clinic, and

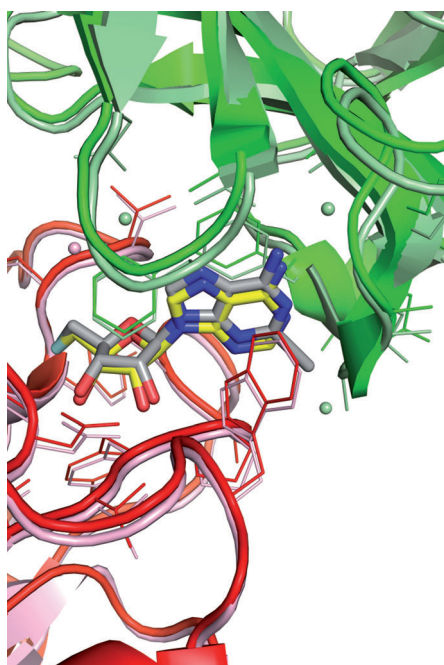
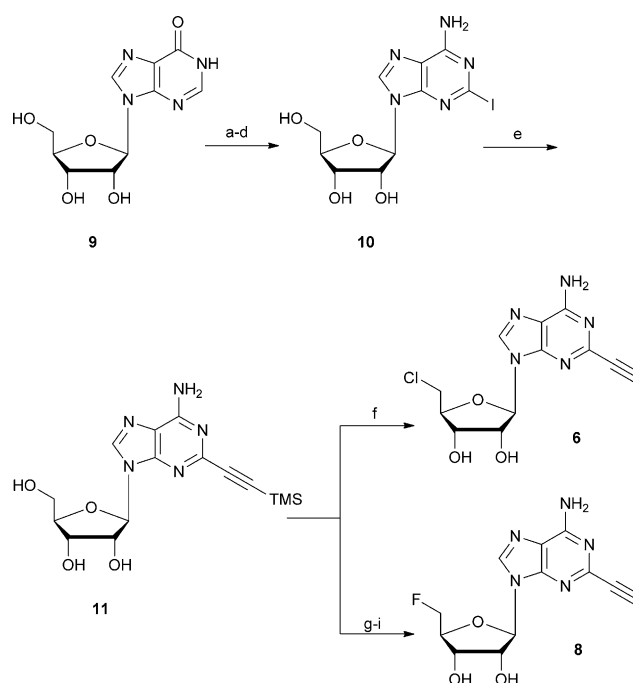


Figure 1. Overlay of co-crystal structures of the fluorinase enzyme with FDA (**2**; yellow, pink, and pale green) and the fluorinase enzyme with FDEA (**8**; gray, red, and bright green). The projection of the acetylene functionality of **8** between two subunits (red and green) of the fluorinase enzyme is shown.

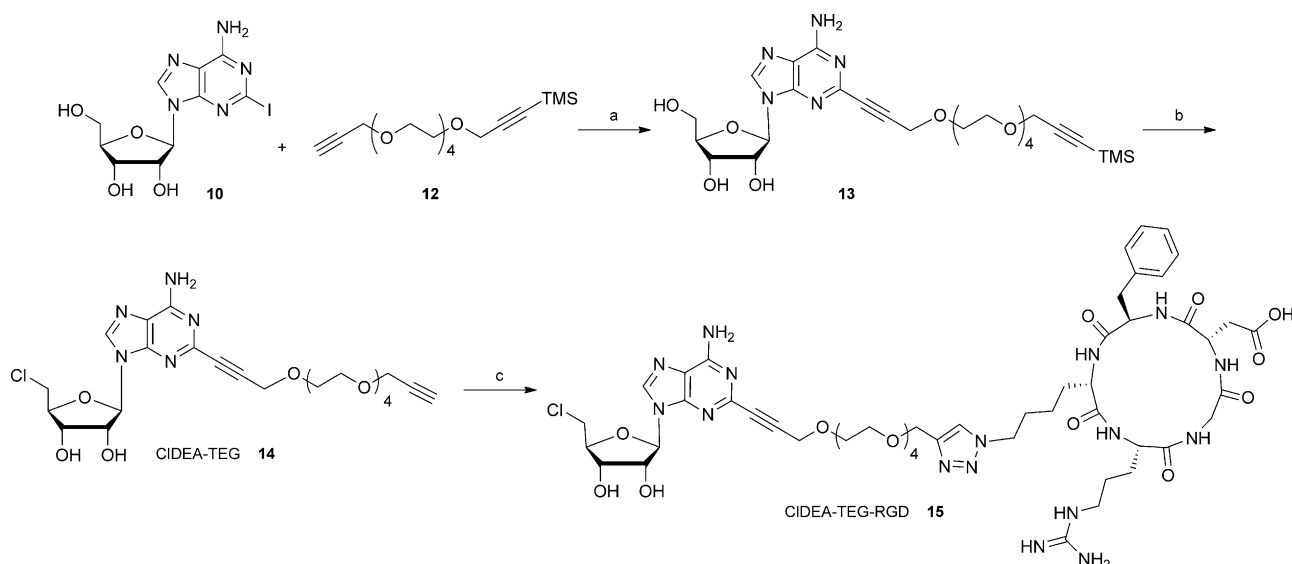
the co-crystal structures of **2** and **8** shows **8** (gray, Figure 1) bound in the active site in a similar manner to FDA (**2**; yellow). The acetylene substituent at the C-2 position of **8** projects into the solvent.

Incubation of CIDEA (**6**) with the fluorinase enzyme and L-SeMet, resulted in the conversion of **6** into FDEA (**8**), as illustrated in Scheme 1 b (for HPLC profiles see Figure S1a in the Supporting Information). The reaction progressed at about 60 % of the rate of conversion of CIDA (**4**) into FDA (**2**,



Scheme 2. Synthesis of CIDEA (**6**) and FDEA (**8**). Reagents and conditions: a) Ac_2O , pyridine, DMF, 84 %. b) POCl_3 , Et_4NCl , dimethylaniline, CH_3CN , 77 %. c) CuI , I_2 , CH_2I_2 , isoamyl nitrite, THF, 69 %. d) NH_3 , MeOH, 69 %. e) $[\text{Pd}(\text{PPh}_3)_2\text{Cl}_2]$, Et_3N , CuI , DMF, trimethylsilylacetylene, 60 %. f) SOCl_2 , pyridine, CH_3CN , then NH_3 , MeOH, H_2O , 47 %. g) 2,2-dimethoxypropane, Amberlyst 15(H^+), 53 %. h) TBAF (tetrabutylammonium fluoride), TsF (tosyl fluoride), THF, 71 %. i) TFA (trifluoroacetic acid), H_2O , 53 %.

so were explored as the model system. To this end, CIDEA-TEG-RGD (**15**, TEG = tetraethylene glycol), emerged as a synthetic target (Scheme 3). The PEG chain was incorporated into the design to project the cyclic peptide into the bulk solvent. A key step involved the Sonogoshira cross-coupling



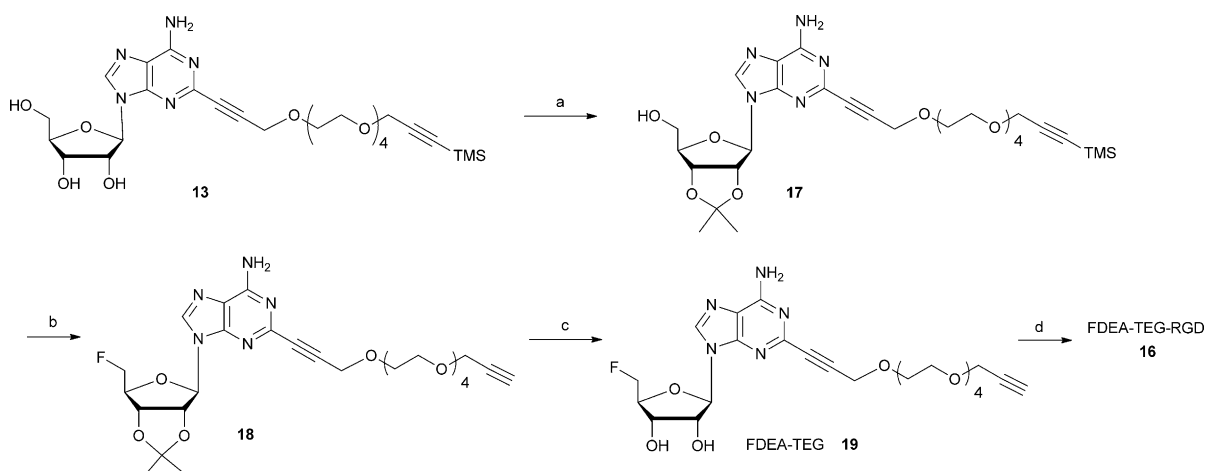
Scheme 3. Synthesis of CIDEA-TEG-RGD (**15**). Reagents and conditions: a) $[\text{Pd}(\text{PPh}_3)_2\text{Cl}_2]$, Et_3N , CuI , DMF , 67%. b) SOCl_2 , pyridine, CH_3CN , then NH_3 (aq), 20%. c) $\text{c(RGDfK(N}_3))$, CuSO_4 -TBTA (TBTA = tris[(1-benzyl-1H-1,2,3-triazol-4-yl)methyl]amine), sodium ascorbate, 67%; where for $\text{c(RGDfK(N}_3))$, f = D-phenylalanine, $\text{K(N}_3)$ = the analogue of lysine where the terminal (or ϵ -) amino is replaced with an azide group.

between alkyne **12** and 2-iodoadenosine (**10**) to generate **13**. Reaction of **13** with thionyl chloride gave CIDEA-TEG (**14**) and a HCl/acetylene addition product (see compound **33** in the Supporting Information). The co-product was readily removed from **14** by preparative HPLC. To attach the RGD peptide, **14** was subject to a “click” reaction with $\text{c(RGDfK(N}_3))$, to generate **15**, a product which was purified by HPLC and fully characterized (Supporting Information). Compound **15** was subsequently incubated with the fluorinase enzyme under the previously established conditions (L-SeMet, fluoride, fluorinase enzyme, pH 7.8) and proved to be a good substrate for transhalogenation to FDEA-TEG-RGD (**16**), as monitored by HPLC (Figure 2). No reaction was observed in the absence of the enzyme.

The identity of **16** was confirmed by both mass spectrometry (Figure S4), and against an authentic reference sample

which was synthesized (Scheme 4). The success of this reaction demonstrates that fluorinase-mediated transhalogenation can be accomplished with a peptide cargo attached to the terminus of the acetylenic functional group at the C-terminus of the peptide. This opens up prospects for attaching a variety of peptides to a CIDEA motif, for direct “last-step” ^{18}F fluorine-labelling using fluorinase catalysis for PET.

As few and efficient radiolabelling transformations are possible as desired in PET radiochemistry, because of the relatively short half-life of the ^{18}F isotope ($t_{1/2} = 109.7$ min). This limitation generally requires that ^{18}F fluoride, generated by the cyclotron from ^{18}O water, is dried by ion-exchange chromatography, and made suitable for nucleophilic chemistry. Water-soluble peptides are most commonly labelled with fluorine-18 after the anhydrous synthesis of reactive small molecules followed by a conjugation to the peptide. These



Scheme 4. Direct synthesis of FDEA-TEG-RGD (**16**). Reagents and conditions: a) 2,2-Dimethoxypropane, HClO_4 , MeOH , 90%. b) TBAF, TsF , 55%. c) $\text{CF}_3\text{CO}_2\text{H}$, $\text{MeOH}/\text{H}_2\text{O}$, 69%. d) $\text{c(RGDfK(N}_3))$, CuSO_4 -TBTA, sodium ascorbate, 70%.

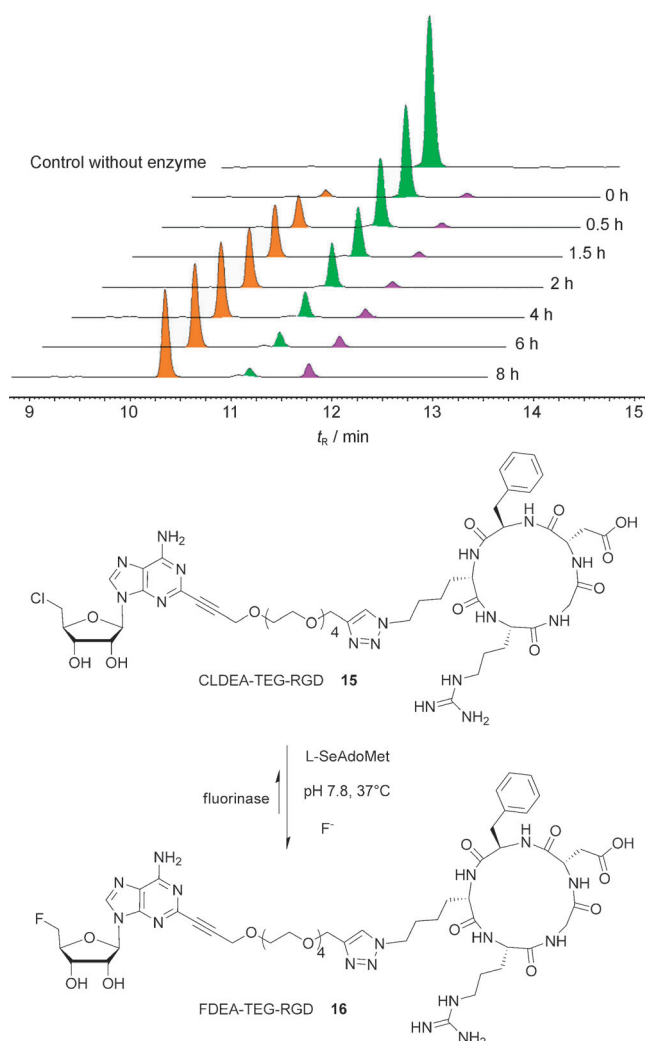


Figure 2. HPLC trace showing the conversion of CLDEA-TEG-RGD (**15**) into FDEA-TEG-RGD (**16**) by the fluorinase enzyme. Conditions: KF, L-SeMet, fluorinase enzyme, phosphate buffer, pH 7.8, 37°C. Traces show the formation of peptide **16** ($t_R = 10.2$ min; orange), while **15** ($t_R = 11.0$ min, green) is consumed. Some accumulation of SeAdoMet is observed, evidenced by the presence of a SeAdoMet breakdown product (purple).

procedures require at least two transformations after isolation of the [^{18}F]fluoride ion by ion-exchange chromatography. However “last-step” fluorination procedures for peptides are less well developed as a result of the incompatibility of peptides with non-aqueous solvents and a requirement for heating to improve the rate of reactions. Current strategies for the direct labelling of peptides have used fluoride-sequestering strategies. Radiolabelled trifluoroborates^[14] have been prepared using aqueous [^{18}F]fluoride and KFH_2 , but at low pH values (pH 2), while aluminum hydroxide complexes^[16] require heating at elevated temperatures (105°C) for fluorination. A silicon-based fluoride-acceptor approach^[15] and direct nucleophilic fluorination reactions^[17,18] at a carbon center require anhydrous conditions and heating to incorporate fluoride substituents. It is in this context that fluorinase enzymatic catalysis presents an attractive strategy for last-

step fluorination of peptides as no drying of the [^{18}F]fluoride is required and reactions occur at ambient temperature and neutral pH in buffer solution.

A transhalogenation reaction was explored with **15** using [^{18}F]fluoride for conversion into [^{18}F]**16**. The reaction progressed at a modest rate under “cold” fluoride ion conditions (non-radiolabelled) as illustrated in Figure 2, however for fluorinase-catalyzed radiochemical reactions, higher product yields can be achieved using very low concentrations of fluoride. The cyclotron generates a solution of [^{18}F]fluoride at picomolar (10^{-12}M) concentration. The fluorinase enzyme is added to this solution at a micromolar (10^{-6}M , 15–20 mg mL^{-1}) concentration, with a 10^6 molar excess of enzyme over fluoride ion in the radiochemical biotransformation. Under these conditions, the enzyme is not catalytic. The success of the radiochemical experiments lies in converting the picomolar aqueous [^{18}F]fluoride into organic [^{18}F]fluorine and generally very good radiochemical conversions are achieved because of the heavily biased stoichiometry. As anticipated, the radiochemical conversion of **15** into [^{18}F]**16** was excellent. Figure 3 shows the simultaneous radiochemical and UV detection HPLC traces of the supernatant of the reaction mixture (30 min, room temperature) after denaturation of the enzyme. The supernatant displays a signal indicating almost complete conversion into [^{18}F]**16** in the radio trace, while the UV trace reveals the excess of **15**. The identity of [^{18}F]**16** was confirmed by examination of HPLC run which had been spiked with cold **16** (see Figure S5).

The ability of peptide **16**^[19] to bind to $\alpha_v\beta_3$ integrins was investigated. It is clear from Table 1 that **16** retains a high affinity for $\alpha_v\beta_3$ integrin in comparison with structurally less elaborate cyclic RGD peptides and has a significantly higher affinity than the RGD motif itself.

Table 1: IC_{50} binding affinity of RGD-containing peptide motifs for immobilized $\alpha_v\beta_3$ integrin.^[a]

Compound	IC_{50} [μM]	Q
RGD	8.56	4.019
c(RGDfK) ^[b]	0.11	0.052
c(RGDfC) ^[b]	0.08	0.038
FDEA-TEG-RGD	0.07	0.033

[a] Q is the normalized activity of the peptides referenced to linear GRGDSPK ($Q = 1$). [b] IC_{50} values reported previously using an identical assay.^[20]

Peptide [^{18}F]**16** was then injected into a healthy rat to investigate its robustness to defluorination. There was some evidence of metabolism of the peptide, however a combination PET/CT (CT = computerized tomography) whole-body images, averaging scans over a 1 h period (Figure 4), did not show radioactivity uptake in the bone. The absence of uptake indicates that **16** is stable to [^{18}F]fluoride ion release, an important prerequisite of a PET radiotracer. The peptide distribution in different organs was assessed after dissection (Figure S7) and had a profile (for example, highest radioactivity in kidney, intestine, spleen, and lung) consistent with distribution of an intact RGD motif.^[21]

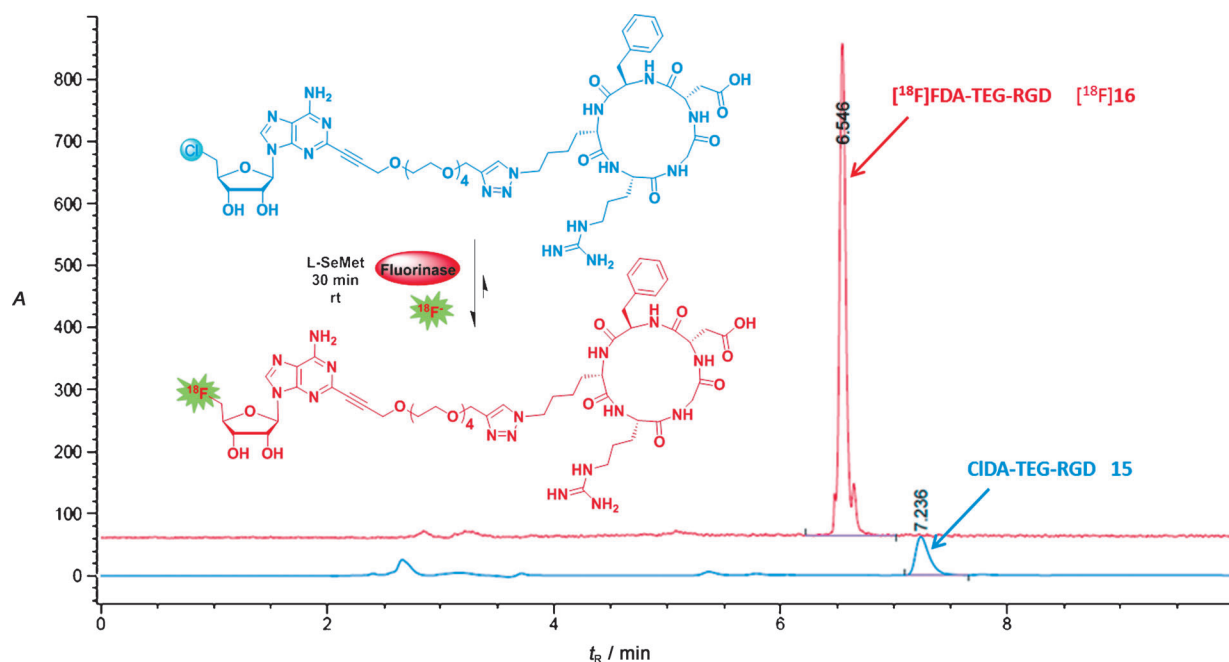


Figure 3. Radiochemical and UV detection HPLC traces for the enzyme-catalyzed transformation of **15** to $[^{18}\text{F}]\mathbf{16}$ (after 30 min, room temperature). Radiochemical-detection trace (red) shows $[^{18}\text{F}]\mathbf{16}$ ($t_R = 6.5$ min); UV-detection trace (blue) shows excess **15** ($t_R = 7.2$ min).

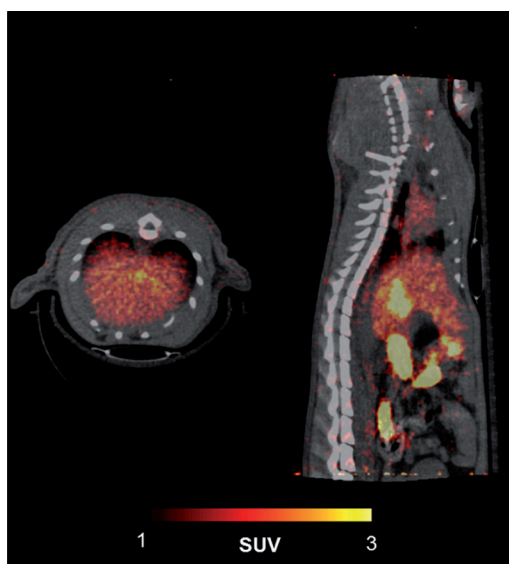


Figure 4. Summed transaxial (left) and sagittal (right) PET images of a rat, 5–60 min following administration of $[^{18}\text{F}]\mathbf{16}$ (5 MBq). PET images are co-registered with corresponding CT images (gray scale). No evidence of bone uptake could be observed, suggesting good in vivo stability of the C–F bond of the 5'- $[^{18}\text{F}]$ fluoro-deoxyadenosine fragment. PET images are presented as standard uptake values ($\text{SUV} = [\text{tissue activity (mL)}] / [\text{injected activity/animal weight (g)}]$).

This study demonstrates a breakthrough in fluorinase enzyme substrate specificity and its application to enzymatic last-step ^{18}F labelling of peptides from aqueous cyclotron-generated $[^{18}\text{F}]$ fluoride. We are currently investigating a range of other peptides and linkers and exploring the metabolism of

such constructs to develop this approach as a strategy for tumor-imaging studies.

Received: March 18, 2014

Published online: July 2, 2014

Keywords: bioconjugated peptides · enzyme catalysis · fluorinase · fluorine-18 · positron emission tomography

- [1] D. O'Hagan, C. Schaffrath, S. L. Cobb, J. T. G. Hamilton, *Nature* **2002**, 416, 279–280.
- [2] S. Dall'Angelo, N. Bandaranayaka, A. D. Windhorst, D. J. Vugts, D. van der Born, M. Onega, L. F. Schweiger, M. Zanda, D. O'Hagan, *Nucl. Med. Biol.* **2013**, 40, 464–470.
- [3] R. Schirmacher, C. Wängler, E. Schirmacher, *Mini-Rev. Org. Chem.* **2007**, 4, 317–329.
- [4] M. Winkler, J. Domarkas, L. F. Schweiger, D. O'Hagan, *Angew. Chem.* **2008**, 120, 10295–10297; *Angew. Chem. Int. Ed.* **2008**, 47, 10141–10143.
- [5] X.-G. Li, S. Dall'Angelo, L. F. Schweiger, M. Zanda, D. O'Hagan, *Chem. Commun.* **2012**, 48, 5247–5249.
- [6] X.-G. Li, J. Domarkas, D. O'Hagan, *Chem. Commun.* **2010**, 46, 7819–7821.
- [7] H. Deng, S. L. Cobb, A. R. McEwan, R. P. McGlinchey, J. H. Naismith, D. O'Hagan, D. A. Robinson, J. B. Spencer, *Angew. Chem.* **2006**, 118, 773–776; *Angew. Chem. Int. Ed.* **2006**, 45, 759–762.
- [8] C. Dong, F. Huang, H. Deng, C. Schaffrath, J. B. Spencer, D. O'Hagan, J. H. Naismith, *Nature* **2004**, 427, 561–565.
- [9] V. Nair, S. Richardson, *Synthesis* **1982**, 670–672.
- [10] A. Matsuda, M. Shinozaki, M. Tadashim, H. Machida, T. Abiru, *Chem. Pharm. Bull.* **1985**, 33, 1766–1769.
- [11] M. J. Robins, F. Hansske, S. F. Wnuk, T. Kanai, *Can. J. Chem.* **1991**, 69, 1468–1474.

- [12] M. Shimizu, Y. Nakahara, H. Yoshioka, *Tetrahedron Lett.* **1985**, 26, 4207–4210.
- [13] H. Cai, P. S. Conti, *J. Labelled Compd. Radiopharm.* **2013**, 56, 264–279.
- [14] Y. Li, Z. Liu, J. Lozada, M. Q. Wong, K.-S. Lin, D. Yapp, D. M. Perrin, *Nucl. Med. Biol.* **2013**, 40, 959–966.
- [15] R. Schirrmacher, G. Bradtmöller, E. Schirrmacher, O. Thews, J. Tillmanns, T. Siessmeier, H. G. Buchholz, P. Bartenstein, B. Wängler, C. M. Niemeyer, K. Jurkschat, *Angew. Chem.* **2006**, 118, 6193–6197; *Angew. Chem. Int. Ed.* **2006**, 45, 6047–6050.
- [16] C. A. D'Souza, W. J. McBride, R. M. Sharkey, L. J. Todaro, D. M. Goldenberg, *Bioconjugate Chem.* **2011**, 22, 1793–1803.
- [17] J. Becaude, L. Mu, M. Karraamkam, P. Schubiger, S. M. Ametamey, K. Graham, T. Stellfeld, L. Lehmann, S. Borkowski, D. Berndorff, L. Dinkelborg, A. Srinivasan, R. Smits, B. Koksche, *Bioconjugate Chem.* **2009**, 20, 2254–2261.
- [18] O. Jacobson, L. Zhu, Y. Ma, I. D. Weiss, X. Sun, G. Niu, D. O. Kiesewetter, X. Chen, *Bioconjugate Chem.* **2011**, 22, 422–428.
- [19] S. Dall'Angelo, Q. Z. Zhang, I. Fleming, M. Piras, L. F. Schweiger, D. O'Hagan, M. Zanda, *Org. Biomol. Chem.* **2013**, 11, 4551–4558.
- [20] M. Piras, I. Fleming, W. Harrison, M. Zanda, *Synlett* **2012**, 2899–2902.
- [21] J. Oxboel, M. Brandt-Larsen, C. Schjoeth-Eskesen, R. Myschetsky, H. H. El-Ali, J. Madsen, A. Kjaer, *Nucl. Med. Biol.* **2014**, 41, 259–267.